

CMB and LSS Power Spectra From Local Cosmic String Seeded Structure Formation

Carlo R. Contaldi¹, Mark Hindmarsh² and João Magueijo¹

¹ *Theoretical Physics, The Blackett Laboratory, Imperial College, Prince Consort Road, London, SW7 2BZ, U.K.*

² *Centre for Theoretical Physics, University of Sussex, Brighton BN1 9QJ, U.K.*

We evaluate the two point functions of the stress energy from the largest string simulations carried out so far. The two point functions are used to calculate the cosmic microwave background (CMB) and cold dark matter (CDM) power spectra from local cosmic string models for structure formation. We find that our spectra differ significantly from those previously calculated for both global and local defects. We find a higher Doppler peak at $l = 400 - 600$ and a less severe bias problem than for global defects. Spectra were obtained for a variety of network energy-decay mechanisms.

KEYWORDS: Cosmology, Cosmic Strings, CMB & LSS power spectra

1. INTRODUCTION

The next few years will see a great increase in the accuracy of the data mapping the CMB temperature and large scale structure (LSS) due to satellite, balloon and ground based experiments. Similarly accurate theoretical predictions from inflation and defect models will be required for direct comparison with the new data. While calculations of structure formation from inflationary models are relatively straightforward, defects, being highly non-linear objects and active sources of perturbations, pose a more challenging problem.

To this end we report on what we believe to be the most complete numerical treatment of local cosmic strings to date. The method we use is based on that described in [1] where it was shown how to use the two point functions (known as the unequal time correlators, or UETCs) measured from defect simulations to calculate the CMB and LSS power spectra. The method was applied to global defects and the results were discouraging for defect models.

In this work we aimed to verify these results in local theories where the calculations are complicated somewhat by considerations on energy conservation and have only been permitted following recent advances in the computer technology at our disposal. The method we used is considerably different from that used in previous local string calculations based on simulations [2] and we believe that the UETC method is justified by causality and scaling arguments in dramatically extending the dynamical range of defect simulations. We also find that some of our UETCs are approximated quite well by those based on an analytical model [3, 4] but others differ quite significantly and in [6] we show how this model can be elaborated to explain the features observed in the simulations.

2. THE CORRELATORS

The perturbations arising from scalar, vector and tensor (SVT) modes are completely decoupled and evolve separately. To calculate the CMB and LSS power spectra efficiently, it is therefore convenient to decompose the source of the perturbations into irreducible components under rotations.

Let $\Theta_{\mu\nu}(\mathbf{x})$ be the defect stress-energy tensor. We may Fourier analyze it

$$\Theta_{\mu\nu}(\mathbf{x}) = \int d^3k \Theta_{\mu\nu}(\mathbf{k}) e^{i\mathbf{k}\cdot\mathbf{x}} \quad (1)$$

and decompose its Fourier components as:

$$\Theta_{00} = \rho^d \quad (2)$$

$$\Theta_{0i} = i\hat{k}_i v^d + \omega_i^d \quad (3)$$

$$\Theta_{ij} = p^d \delta_{ij} + \left(\hat{k}_i \hat{k}_j - \frac{1}{3} \delta_{ij} \right) \Pi^S + i \left(\hat{k}_i \Pi_j^V + \hat{k}_j \Pi_i^V \right) + \Pi_{ij}^T \quad (4)$$

with $\hat{k}^i \omega_i^d = 0$, $\hat{k}^i \Pi_i^V = 0$, $\hat{k}^i \Pi_{ij}^T = 0$, and $\Pi_i^{Ti} = 0$. The variables $\{\rho^d, v^d, p^d, \Pi^S\}$ are the scalars, $\{\omega_i^d, \Pi_i^V\}$ the vectors, and Π_{ij}^T the tensors.

The unequal time correlators of these components will completely specify the evolution of the network's stress-energy. All correlators between modes at (\mathbf{k}, η) and (\mathbf{k}', η') will be proportional to $\delta(\mathbf{k} - \mathbf{k}')$ due to translational invariance. We shall drop this factor in all formulae. The correlators can also be functions of k alone, due to isotropy. Since conjugation corresponds to $\mathbf{k} \rightarrow -\mathbf{k}$ isotropy implies that the correlators must be real. Because of incoherence the correlators will be generic functions of η and η' .

On top of this, the form of the S+V+T decomposition fixes further the form of the correlators. One can always write down the most general form of a correlator, and then contract the result with \hat{k}_i or δ_{ij} , wherever appropriate, to obtain further conditions. Proceeding in this way we can show that cross correlators involving components of different type (S, V, or T) must be zero. Furthermore one has that the only non-zero correlators are the 10 scalar correlator functions

$$\begin{array}{cccc} f\rho^d\rho^d & f\rho^d v^d & f\rho^d p^d & f\rho^d \Pi^S \\ \dots & f v^d v^d & f v^d p^d & f v^d \Pi^S \\ \dots & \dots & f p^d p^d & f p^d \Pi^S \\ \dots & \dots & \dots & f \Pi^S \Pi^S \end{array} \quad (5)$$

the 3 vector correlators:

$$\begin{array}{cc} f\omega^d \omega^d & f\omega^d \Pi^V \\ \dots & f\Pi^V \Pi^V \end{array} \quad (6)$$

and the single tensor correlator function $f^{\Pi^T\Pi^T}$.

In general these functions are functions of (k, η, η') , and this is indeed the case during the matter radiation transition. However well into the matter and radiation epochs there is scaling, and these functions may be written as:

$$f^{XY}(k, \eta, \eta') = \frac{F^{XY}(x, x')}{\sqrt{\eta\eta'}} \quad (7)$$

where XY represents any pair of superscripts considered above, and $x = k\eta$ and $x' = k\eta'$. The purpose of this work is the measurement of the 14 functions of two variables $F^{XY}(x, x')$.

3. NUMERICAL DETERMINATION OF THE CORRELATORS

Local strings have an extra complication over global defects, which stems from the fact that we are unable to simulate the underlying field theory. Instead, we approximate the true dynamics with line-like relativistic strings using the Nambu equations of motion. We used a previously developed implementation [5, 7] of this algorithm which simulates the network of strings neglecting damping effects due to the expansion of the Universe. The velocities of the strings segments in the network can be constrained to be integers due to the gauge conditions used to discretise the equations of motion and this enables the code to obtain very high accuracy with extremely fast computation.

To simulate the extraction of energy from the system due to the decay of the string loops into gravitational radiation, loops of a minimum size are excised from the simulation at each timestep. This also ensures that the network scales with respect to the conformal time η which enables us to extend the dynamical range of the resulting correlation functions beyond the limited range covered in the simulation.

We performed simulations with box sizes ranging from 128^3 to 600^3 , with a cut-off on the loop size of two links. Realisation averages were carried out with 256^3 boxes once it was determined that the general form of the correlators scaled very accurately with box size. To evaluate the UETCs from the simulations we selected times in the range $0.1N < t < N/4$, where N is the box size, when we were sure that the string network was scaling, and when boundary effects are still excluded by causality. From this we obtained the time evolution of the network's stress-energy tensor $\Theta_{\mu\nu}$ at each point on the lattice using

$$\Theta_{\mu\nu}(\mathbf{x}) = \mu \int d\sigma (\dot{X}^\mu \dot{X}^\nu - \dot{X}^\mu \dot{X}^\nu) \delta^3(\mathbf{x} - \mathbf{X}(\sigma, \eta)) \quad (8)$$

where $X(\sigma, \eta)$ is the spacetime coordinate of the string with σ a parameter along the string. SVT decomposition was carried out on the 10 independent components of the Fourier transform of the stress-energy tensor at each timestep. This resulted in all the SVT components being computed directly from the simulation without

making assumptions on energy conservation and on the details of energy dissipation from the string network. The drawback of obtaining all the components directly in such a manner is that the process becomes computationally intensive for even modestly sized simulations e.g. 256^3 . By cross-correlating the decomposed stress-energy components from a central time with those from all the stored timesteps the 14 independent UETC's $f^{XY}(k, \eta, \eta')$ were computed.

Standard codes for structure formation [10] require the square root of coherent correlators for sourcing the inhomogeneous differential equations but this is not straightforward in general defect scenarios because the correlators are incoherent and therefore do not factorise. To overcome this, following [1], we expand the matrix of scaling functions onto a basis of coherent functions $v_{\alpha\beta}^{(i)}(k\eta)$ by diagonalising the matrix of correlators

$$c_{\mu\nu,\alpha\beta}(k\eta, k\eta') = \sum_i \lambda^{(i)} v_{\mu\nu}^{(i)}(k\eta) v_{\alpha\beta}^{(i)}(k\eta') \quad (9)$$

where $\lambda^{(i)}$ are eigenvalues. Each coherent, weighted eigenmode is then fed into the standard codes and the total C_l and $P(k)$ are then the convergent sums of the resulting components.

4. RESULTS

The most striking difference between our work on local strings and previous work on global defects is that we find the Θ_{00} term comes to dominate over all the other components and thus vector and tensor components contribute much less significantly in our results. The string anisotropic stresses are in the predicted [8] ratios $|\Theta^S|^2 : |\Theta^V|^2 : |\Theta^T|^2$ of $3 : 2 : 4$, as $k\tau \rightarrow 0$, however $|\Theta_{00}|^2 \gg |\Theta^S|^2$. Also we find that the peak in the energy density power spectra occurs at $k\tau \approx 20$ which is well inside the horizon. In general this leads to a higher Doppler peak than observed in [1, 4].

For a full treatment we must also include in the calculations the background fluid into which the network of strings dumps energy. One of the greatest unknowns in the dynamics of cosmic strings is the channel through which this energy is discarded and this is quantified by assuming an equation of state for the extra fluid, of the form $p^X = w^X \Theta_{00}^X$, where w^X is varied in the range $0 < w^X < 1/3$ so as to account for the non-relativistic case through to the relativistic case.

In Fig.1 we plot $\sqrt{[\ell(\ell+1)C_\ell/2\pi]}$, setting the Hubble constant to $H_0 = 50 \text{ Km sec}^{-1} \text{ Mpc}^{-1}$, the baryon fraction to $\Omega_b = 0.05$, and assuming a flat geometry, no cosmological constant, 3 massless neutrinos, standard recombination, and cold dark matter. The most interesting feature is the presence of a reasonably high Doppler peak at $\ell = 400 - 600$, following a pronouncedly tilted large angle plateau. This feature sets local strings apart from global defects. It puts them in a better shape to face the current data.

In Fig.2 we plotted the CDM power spectrum $P(k)$ together with experimental points as in [9]. The normalization has been fixed by COBE data points. We

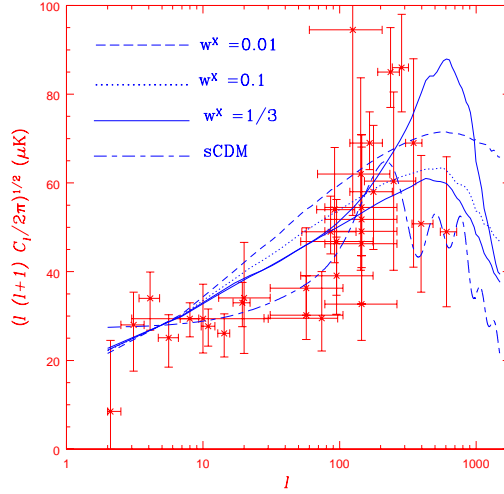


Fig.1 The CMB power spectra predicted by cosmic strings decaying into loop and radiation fluids with $w^X = 1/3, 0.1, 0.01, 0$. We have plotted $(\ell(\ell + 1)C_\ell/2\pi)^{1/2}$ in μK , and superposed several experimental points.

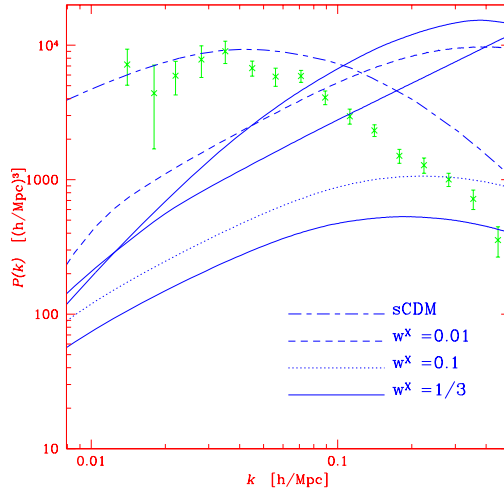


Fig.2 The power spectrum in CDM fluctuations for cosmic strings, with $w^X = 0.01, 0.1, 1/3$. We plotted also the standard CDM scenario prediction and points inferred by Peacock and Dodds from galaxy surveys.

see that the peak of the spectrum is always at smaller scales than standard CDM predictions, or observations. The CDM rms fluctuation in $8 h^{-1}\text{Mpc}$ spheres is $\sigma_8 = .42, .61, 1.8$ for $w^X = 1/3, 0.1, 0.01$. Hence relativistic decay products match well the observed $\sigma_8 \approx 0.5$. On the other hand in $100 h^{-1}\text{Mpc}$ spheres one requires bias $b_{100} = \sigma_{100}^{data}/\sigma_{100} = 4.9, 3.7, 1.6$ to match observations.

In this work we have calculated the CMB and LSS power spectra arising from local cosmic string scenarios using the largest string simulations to date. The spectra account for a variety of energy decay mechanisms and the result we want to highlight is the significant difference between structure formation processes arising from global and local defects which show that the $100 h^{-1} \text{Mpc}^{-1}$ bias problem and low Doppler peaks are not as generic effects as was previously thought.

ACKNOWLEDGMENTS We thank A. Albrecht, R. Battye and P. Ferreira for useful discussions. Special thanks are due to U-L. Pen, U. Seljak, and N. Turok for giving us their global defect UETCs, and to P. Ferreira for letting us use and modify his string code. This work was performed on COSMOS, the Origin 2000 supercomputer owned by the UK-CCC and supported by HEFCE and PPARC. We acknowledge financial support from the Beit Foundation (CRC), PPARC (MH), and the Royal Society (JM).

REFERENCES

References

- [1] U-L. Pen, U. Seljak, N. Turok, Phys.Rev.Lett. **79** (1997) 1611-1614.
- [2] B. Allen et al, Phys.Rev.Lett. **79** (1997) 2624-2627.
- [3] G. Vincent, M. Hindmarsh, and M. Sakellariadou, Phys.Rev. **D55** 573-581 (1997).
- [4] A. Albrecht, R. Battye, J. Robinson, Phys.Rev.Lett. **79** (1997) 4736-4739.
- [5] D. Coulson, P. Ferreira, P. Graham, and N. Turok, Nature **368**, 27-31 (1994).
- [6] C. Contaldi, M. Hindmarsh, J. Magueijo, in preparation.
- [7] A. Smith and A. Vilenkin, Phys.Rev.**D36** 990 (1987).
- [8] N. Turok, U-L. Pen, U. Seljak, Phys.Rev. **D58** (1998).
- [9] J. Peacock and S. Dodds, *M.N.R.A.S.* **267** 1020 (1994).
- [10] U. Seljak and M. Zaldarriaga, *Astrop.J.* **469**, 437 (1997).